

MICRON SIZE LASER-WIRE SYSTEM AT THE ATF EXTRACTION LINE*

A. Aryshev[†], G. A. Blair, S. T. Boogert, G. Boorman, A. Bosco, L. Deacon, P. Karataev (John Adams Institute at RHUL, London, UK), D. Howell, L. J. Nevey, L. Corner, N. Delerue, B. Foster, F. Gannaway, M. Newman, R. Senanayake, R. Walczak (John Adams Institute at Oxford, UK), H. Hayano, N. Terunuma, J. Urakawa (KEK, Ibaraki, Japan)

Abstract

The KEK Accelerator test facility (ATF) extraction line laser-wire system has recently been upgraded allowing the measurement of micron scale transverse size electron beams. We report on the hardware upgrades, including focusing lens, laser diagnostics and mechanical systems. The first measurements using the new system from recent operation at the ATF are presented.

INTRODUCTION

The requirement for non-invasive diagnostics, such as transverse profiling of charged particles beams is well established. Such diagnostic devices should have high reliability, resolution and comparative simplicity in use. The primary advantages of Laser-wire (LW) compared with screens and conventional wire scanners are its negligible impact on the charged particle beam, a higher resolution and possibility of fast scanning [1].

The basic principle of the ATF extraction line LW monitor is to deliver a strongly focused laser beam at right angles to the electron beam, as shown in Figure 1. When the

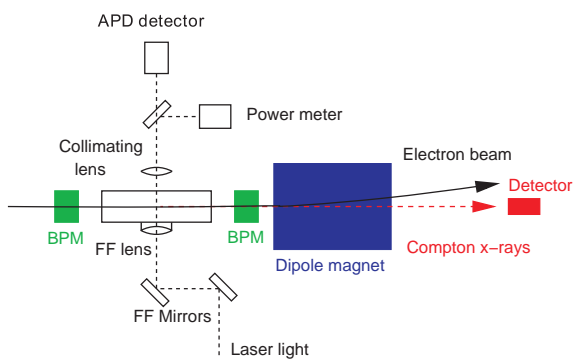


Figure 1: Schematic plan of the interaction region.

electron beam crosses the laser beam, some of the electrons interact with the laser light via the Compton scattering process, resulting in energetic photons in the electron propagation direction. A detector placed downstream of the collision point measures the flux of the scattered photons. By

*Work supported in part by the STFC LC-ABD Collaboration, the Royal Society, the Sasakawa Foundation, and by the Commission of European Communities under the 6th Framework Programme Structuring the European Research Area, contract number RIDS-011899

[†] alar@post.kek.jp

moving the position of the laser focus across the electron beam while measuring the signal count rate, a transverse profile of the electron beam is obtained. Provided both the beams have gaussian distributions (and neglecting the laser divergence) the measured profile width (σ_y) is the quadratic sum of the electron beam width (σ_e) and laser beam with ($\sigma_l = W_0/2$)¹, so $\sigma_y = \sqrt{\sigma_e^2 + \sigma_l^2}$.

In this paper we present the changes made to the LW setup in the last year since we last reported [2, 3], and the most recent calculations and experimental results.

EXPERIMENTAL SETUP

The LW setup is located at the ATF extraction line [4] where a special set of electron beam optics has been developed to generate a suitable beam size at the LW location [5]. The ATF, laser system, gamma ray detectors, timing system and DAQ system are largely unchanged and will not be discussed further [2, 3]. The main upgrade was the installation of a custom $f/2$ focusing lens which, in principle allows the system to reach the goal of $1\mu\text{m}$ transverse beam size measurements. In order to achieve the small laser spot size at the focus the custom designed and built triplet lens, shown in Figure 2, is used. The lens consists of three fused silica elements, an aspheric, spherical and flat (which acts as the vacuum window), all coated with an ultra-high damage threshold and hard anti-reflection coating. The lens has a effective focal length of 56.6 mm.

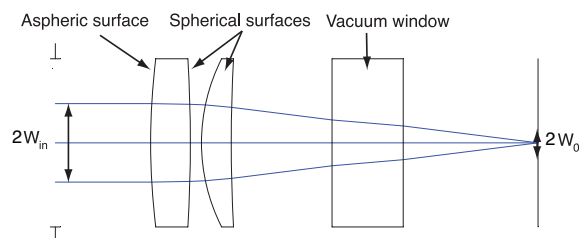


Figure 2: Schematic design of the aspheric lens. The W_{in} is the transverse laser beam radius and the W_0 is the minimal spot size at the focus.

In order to maintain precise alignment the lens is rigidly mounted to the vacuum chamber, which means that in order

¹Conventionally laser beam radii are measured from the peak irradiance to the point at which the irradiance distribution reaches $1/e^2$ of its peak value, denoted W

to move the laser focus with respect to the electron beam in the vertical (y) and in horizontal (x) directions the whole chamber must be moved (see Fig. 3). To be able to position the chamber with sub-micron accuracy stepping motors with $100x$ reduction gear-boxes were employed.

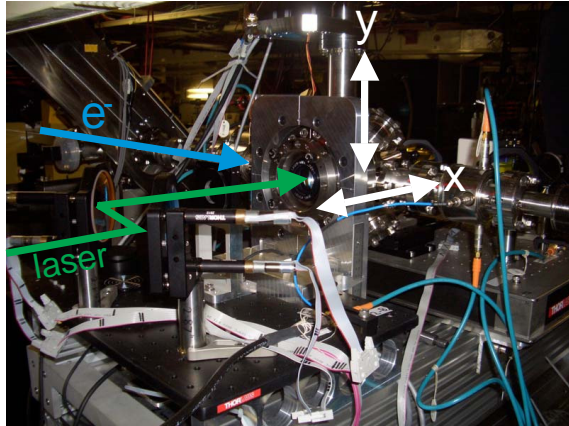


Figure 3: Photograph of the IP chamber with two final steering mirrors and $f/2$ lens.

LASER OPTICS

Laser Diagnostics

A sampling beam-splitter was incorporated in the high-power laser path for laser diagnostics measurements. The low-power split beam was again split into two separate diagnostics beam paths for measurement of M^2 and the input laser beam size.

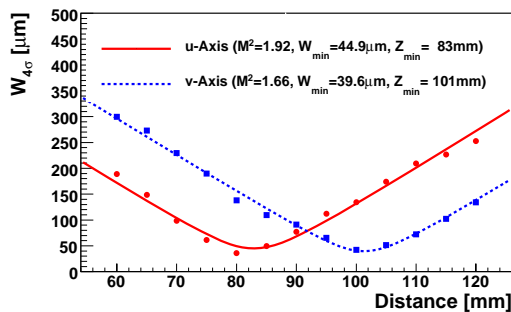


Figure 4: Laser beam radius as a function of distance from the 1 m focal length diagnostics lens.

The factor M^2 is a parameter that describes the laser beam quality, it characterises how close to diffraction limit it is possible to focus a laser. As a laser beam passes through various optical elements it experiences distortions of wave front leading to increase of M^2 . One beam was focused by 1 m plano-convex lens toward a special laser-profiling CCD-camera that could be translated along the laser beam propagation direction. Figure 4 shows the laser

image radius as a function of distance from the lens along with the calculated M^2 parameters for the two orthogonal planes (denoted u and v), the u -plane is orientated at 23.7° from the horizontal (y) axis. According to this measurement the laser beam is significantly astigmatic and its propagation different in two orthogonal planes.

In the second diagnostics path the laser beam is incident onto a paper screen marked with a calibration pattern. The screen was imaged by a second laser-profiling CCD-camera via a standard camera lens. The radius W_{in} was found to be approximately 8.5 mm.

Lens Performance

The $f/2$ lens was both simulated using ZEMAX [6] and also measured in an optical test bench. The simulations used the physical optics propagation (POP) mode of ZEMAX to simulate the passage of a lowest order Gaussian laser mode (TEM_{00}) through the lens to the focus. The beam radius was calculated at various distances from the focus and used to compute the focus radius and the M^2 of the laser, shown in Figures 5 and 6 respectively. The simulation is compared with measurements of the focus produced by the lens of a near perfect, $M^2 = 1$ continuous wave laser. The focus is measured using a rotating drum knife edge scanner specifically designed to measure micron size foci.

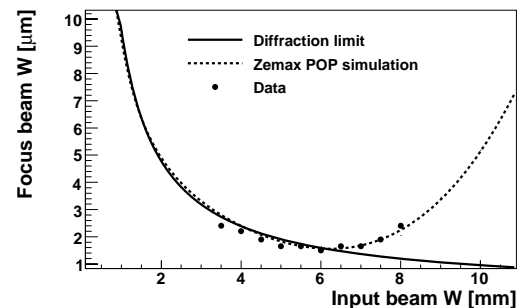


Figure 5: Focus radius of the $f/2$ lens as a function of input laser beam radius.

RESULTS

The results presented here are from a single experimental shift during May 2008. The electron beam focus was again confirmed by making beam size measurements by a wire scanner, consisting of a $10 \mu\text{m}$ tungsten wire which could be scanned across the electron beam and located 0.63 m upstream from the LW interaction point. The vertical beam size at the wire scanner location was again confirmed to be less than the vertical wire scanner resolution limit $2.5 \mu\text{m}$.

Due to the strong laser focusing optics, the laser Rayleigh range is relatively small (about $20 \mu\text{m}$), it is essential that the laser-beam waist is located centrally on the electron beam. In order to achieve these conditions the two

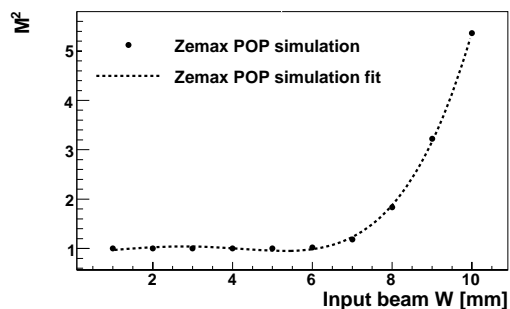


Figure 6: M^2 after the $f/2$ lens as function of input beam radius (W_{in})

preliminary chamber scans (vertical and horizontal)² were always performed before a "measurement" vertical scan. An example of a vertical scan at the laser waist is shown in Figure 7. The signal peaks were fitted to the sum of a Gaussian and linear function. Clearly from figure 7 there are large tails inconsistent with the Gaussian fit shown, these are almost certainly due to the short Rayleigh range of the laser focus, see [7] for details. Detailed numerical fits need to be performed using the laser and lens data presented in the previous section in order to quantitatively understand spatial overlap of the electron and laser beams.

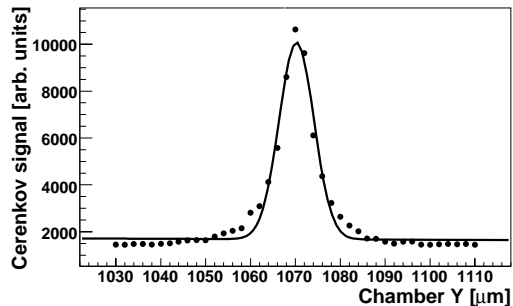


Figure 7: An example of a vertical chamber scan, fitted to sum of Gaussian and linear function.

The laser was moved vertically in steps of $2 \mu\text{m}$ and the Compton signal was recorded for 5 machine cycles at each position step and averaged. The pulse-by-pulse beam charge as well as the laser power was also monitored. In order to minimise the contribution of the electron beam size a quadrupole scan of an upstream quadrupole (QD4X) was performed to set the electron beam waist at the laser wire interaction point. The width (σ_y) of the measured signal Gaussian is plotted as a function of the QD4X magnet current in Figure 8. In addition to optimising the strength of QD4X, two skew quadrupoles QS1X and QS2X were varied and LW scans were performed. In order to investi-

²The purpose of the preliminary scans was to align the laser focus to the center of the electron beam.

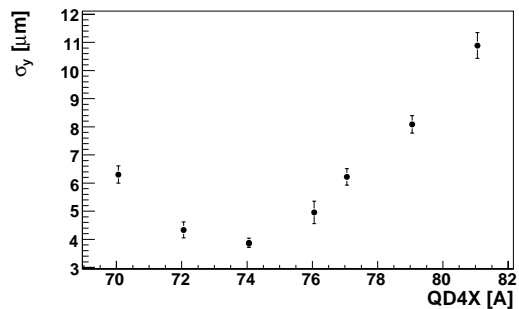


Figure 8: The width (σ_y) of the measured Gaussian as a function of the QD4X magnet strength.

gate the effect of possible horizontal and vertical electron beam coupling. This yielded a minimum signal width of $\sigma_y = 3.7 \mu\text{m}$, although QS1X had to be set to its current limit.

DISCUSSION

The minimum measured profile width was $\sigma_y = 3.7 \mu\text{m}$. According to the calculations for an input laser beam radius of $W_{in} = 8.5 \text{ mm}$ the minimal spot size in focus is $W_0 = 2\sigma_0 = 3 \mu\text{m}$. Given the measured laser M^2 of ~ 1.8 and the astigmatism observed, the measurements of the minimum electron beam size are probably dominated by the laser transverse mode. In order to verify the focus quality and the details of the laser-electron beam overlap an integrated physical optics propagation model including the laser diagnostics data and the lens performance simulations presented here needs to be developed. In this paper we have presented all the data required to perform such an analysis. Alternatively the laser can be modified to remove the astigmatism and hence increase the performance. Another possible solution would be to an alternative laser such as that being developed for linear collider diagnostics [8], or another with better transverse mode quality. The ATF has now finished operation until the autumn 2008, at which time the LW system will be reinstalled in a new location with significantly improved electron optics conditions.

REFERENCES

- [1] A. Bosco *et al.* PAC07, June 2007, Albuquerque, US, p. 422.
- [2] S. T. Boogert *et al.*, EPAC06, June 2006, Edinburgh, UK, p. 738.
- [3] L. Deacon *et al.*, PAC07, June 2007, Albuquerque, US, p. 2636.
- [4] ATF: Accelerator Test Facility Study Report JFY 1996-1999, H. Hayano *et al.* KEK-INTERNAL-2000-6
- [5] S. T. Boogert *et al.*, in preparation
- [6] ZEMAX, <http://www.zemax.com>
- [7] I. Agapov *et al.* Phys. Rev. ST-AB **10** 112801 (2007)
- [8] L. Corner *et al.* in these proceedings